Vol.20, No. 2, Summer 1391/2012

Pages 25 to 32

# Microstructural analysis of quartz crystals in an andalusite-cordierite schist using electron backscatter diffraction

**A. Rahimi-Chakdel[1*], A. P. Boyle[2]**

1- *Department of Geology, Faculty of Science, Golestan University, Gorgan, Iran*
2- *Department of Earth Sciences, University of Liverpool, Liverpool, L69 3GP, U.K*

(Received: 10/1/2011, in revised form: 15/5/2011)

**Abstract:** The present study investigates the shape preferred orientation (SPO) and crystal preferred orientation (CPO) of quartz crystals using electron backscatter diffraction (EBSD) in andalusite-cordierite schist from the Ythan Valley, Aberdeenshire, in the Scottish Dalradian block. Quartz crystals in the matrix and andalusite pophyroblasts have inequant to slightly equant shapes. Quartz crystals show weak SPO in the matrix and andalusite pophyroblasts, which are sub-parallel to each other. The weak SPO in quartz crystals of the studied sample can be related to (1) Grain boundary migration of quartz crystals and (2) non-quartz crystals (e.g. mica) at junction of quartz crystals. Also, quartz crystals show random CPO in the matrix and inclusion. The lack of CPO of quartz crystals in the matrix can be explained by (i) absence, or low amounts of strain in the rock that is experienced only low temperature and pressure and (ii) diffusion creep. The random crystallographic orientation of quartz inclusions may confirm non-selective orientations of the matrix quartz crystals by andalusite pophyroblast during growth.

**Keywords:** *EBSD; Quartz; Shape preferred orientation and crystal preferred orientation*



## Introduction

This study is primarily concerned with a microstructural analysis of quartz crystals in andalusite porphyroblasts and their matrix in an andalusite-cordierite schist from the Aberdeenshire Valley part of the Scottish Dalradian block (Fig. 1). The Scottish Dalradian rocks have been the subject of many classic metamorphic and structural investigations [e.g. 1- 4] that have made major contributions to the understanding of orogenic activities [5].

The Scottish Dalradian is divided into two major provinces on the basis of mineral assemblages at the pelitic rocks [3]. The two provinces are thought to be broadly coeval [6] with the climax of porphyroblast growth occurring between the Barrovian $D_2$ and $D_3$ [2] or Buchan $F_2$ and $F_3$ [6] deformations.

Hudson [4] presented regional metamorphic zones, based on mineral assemblages in pelites for the Dalradian rocks of Aberdeenshire and Banffshire, in the type area of Buchan metamorphism. Read [7] stated that…" the Buchan type of this area is plutonism in which temperature control is main dominant; many of the so-called "antistress" minerals are regionally developed and the country-rock portions of the migmatites are hornfelsic in character". Sample in this study has experienced Buchan-style metamorphism [4].

The present study analyses of collected data on shape preferred orientation (SPO) and crystal preferred orientation (CPO) of quartz crystals using electron backscatter diffraction (EBSD) which may lead to a more fundamental understanding of the controlling factors involved in quartz crystallization[8, 9].

## Analytical Techniques

The sample has been studied from both the geometrical and crystallographic aspects using

* Corresponding author, Tel: (0171) 4427173, Fax: (0171) 4427040, Email: rahimiaz@yahoo.co.uk

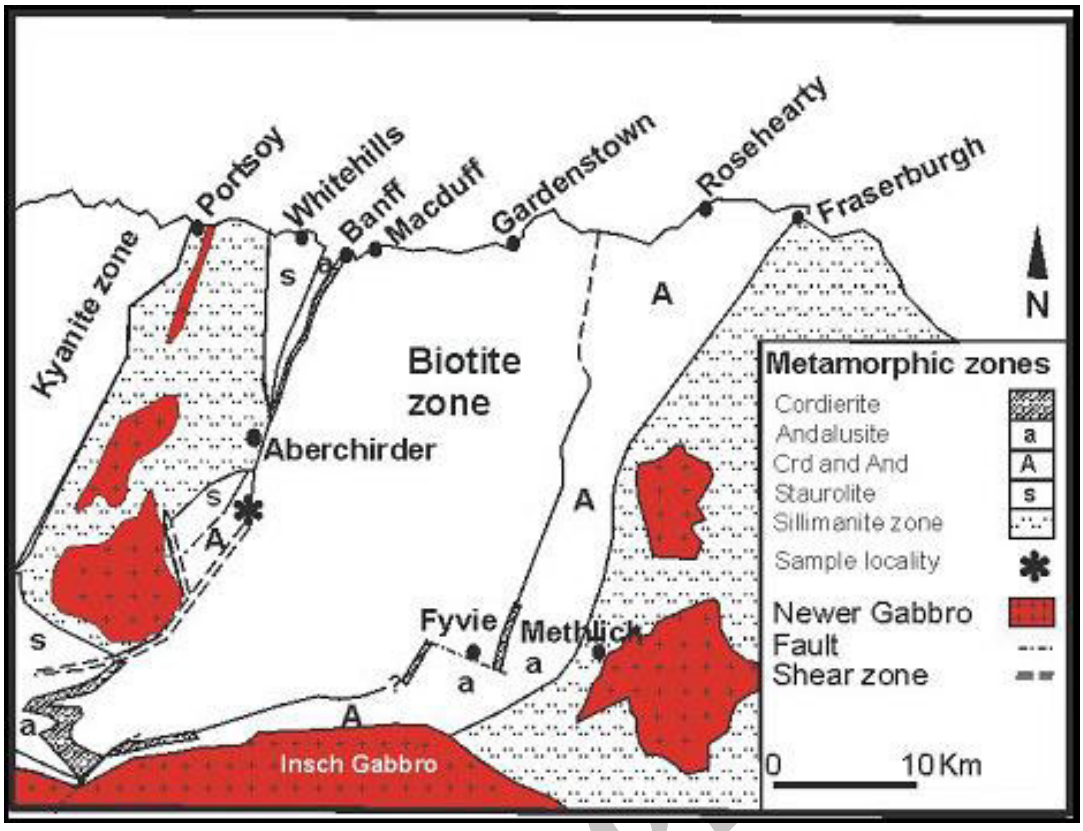


**Figure 1.** Distribution of pelitic metamorphic zones and isograds in the Dalradian of Buchan (after Hudson, 1980). Sample locality illustrated as asterisk.

light microscopy, backscatter electron (BSE) images and EBSD data. BSE images were used to determine shape preferred orientations (SPO), whereas EBSD data were used to quantify crystallographic orientation of quartz grains in inclusions and the rock matrix.

All crystallographic orientations were collected by EBSD on a Philips XL30 (operating software version 4.2) scanning electron microscope (manually) at Liverpool University [8]. In the Philips XL30 SEM, the polished specimen surface is inclined at 70° to the incident beam. An accelerating voltage of 20 kV and a working distance (WD) of 23mm (±0.2 mm), measured to the centre of the image, were used.

Spot sizes (Sp) refer to codes used by the Philips operating system [10]. At 20 kV accelerating voltage and a WD of 20 mm these correspond to beam currents of approximately: Sp5 = 0.8 nA, Sp6 = 3.2 nA, Sp7 = 13.2 nA. Sp5 is typically used for imaging and Sp7 for EBSD [10].

EBSD patterns were imaged on a phosphor screen, viewed by a low light SIT Camera and indexed using the software package CHANNEL$^{+}$4. For each indexed grain, a simulated pattern was compared manually to the EBSD pattern to ensure that computer indexing had calculated the correct orientation [11]. The spatial and angular resolutions of this technique are typically better than 1μm and 1°, respectively.

## Results

### Mineralogy of sample

The mineral assemblage of sample comprises andalusite + cordierite + quartz + muscovite + biotite + plagioclase + epidote + opaque. Andalusite porphyroblasts are 2 to 6 mm in length, typically subhedral in shape and are fresh. Andalusite porphyroblasts commonly occur in close association with cordierite porphyroblasts in this sample. In general, andalusite occurs as thin stringers between and around cordierite porphyroblasts (Figs. 2,3). Locally, andalusite porphyroblasts enclose cordierite suggesting a time sequence of growth. It is also notable that the porphyroblasts (andalusite and cordierite) are always separated from each other by a mosaic of granoblastic polygonal mineral grains composed of quartz with biotite and in some cases plagioclase. All andalusite crystals contain an abundance of inclusions of quartz and tiny biotite and minor

opaque minerals. The inclusions often are straight. Inclusion trails are always continuous with the main matrix schistosity ($S_1$). $S_1$ schistosity was overprinted in some places by andalusite porphyroblasts. The matrix predominantly consists of fine-grained quartz and feldspar and often shows decussate arrangement of white mica. Cordierite grains occur usually 3 or 5 mm in length. The cordierite is commonly completely altered to a fine-grained aggregate of pinite and white micas. These fine-grained minerals are very abundant and show low relief and very low birefringence in thin section. Quartz grains as inclusions define an internal fabric ($S_i$) in the andalusite porphyroblasts. Quartz inclusions have inequant to slightly equant shapes and typically comprise single crystals. Quartz crystals in the matrix are inequant to slightly equant in shape. They show weak alignment in some places that is parallel to a weak foliation around the cordierite porphyroblasts in the rock. Non-quartz minerals (e.g. mica) are at the junction of quartz crystals in the matrix (Fig.4). Quartz-mica (e.g. muscovite) junction is straight with the quartz crystals approximately elongated along this boundary in comparison to the shorter and more irregular quartz-quartz boundaries. Both quartzes in the matrix and porphyroblast show no undulose extinction or deformation lamellae suggesting that they are strain-free.

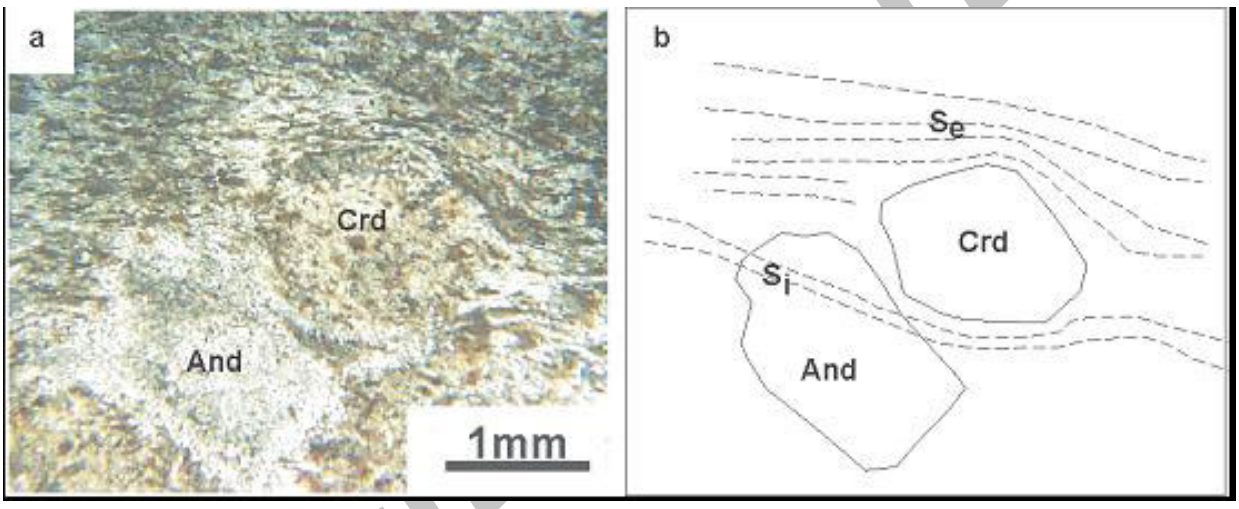


**Figure 2.** PPL image of andalusite-cordierite schist (a) shows weak schistosity that is illustrated in the sketch (b). And = andalusite, Crd = cordierite, $S_e$= external fabric and $S_i$= internal fabric

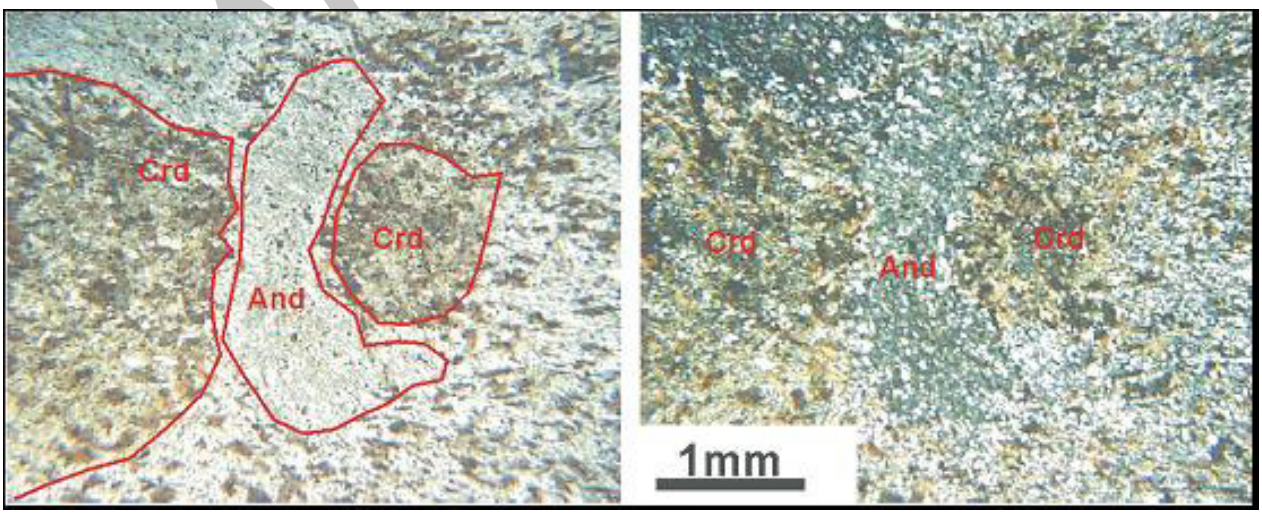


**Figure 3.** PPL (left) and XPL (right) images show an andalusite (And) crystal that partially encloses as stringers between cordierite (Crd).

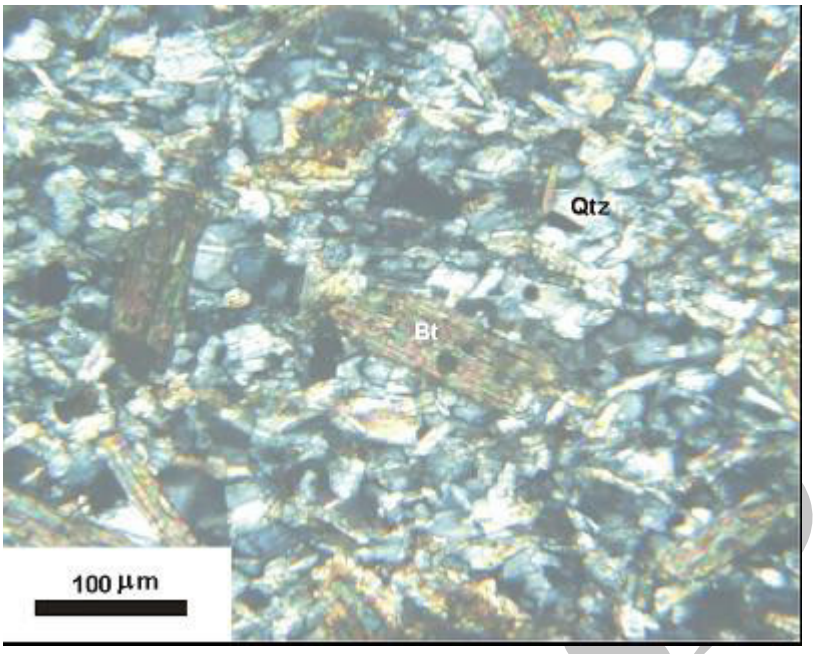


**Figure 4.** XPL image shows quartz grains in the matrix between to non-quartz minerals. Bt = biotite and Qtz = quartz.

**Microstructural analysis using BSE images and EBSD**

**SPO of the matrix quartz crystals using BSE images**

425 long-axes of quartz grains were measured to determine SPOs in the matrix. The orientation data are plotted as a rose diagram (Fig. 5a).

**SPO of quartz crystals in andalusite porphyroblast using BSE images**

139 long-axes of quartz inclusions were measured to determine SPOs in andalusite porphyroblast. The rose diagram plot shows weak SPO of quartz crystals in the porphyroblast, which is approximately sub-parallel to the matrix direction (Fig. 5b).

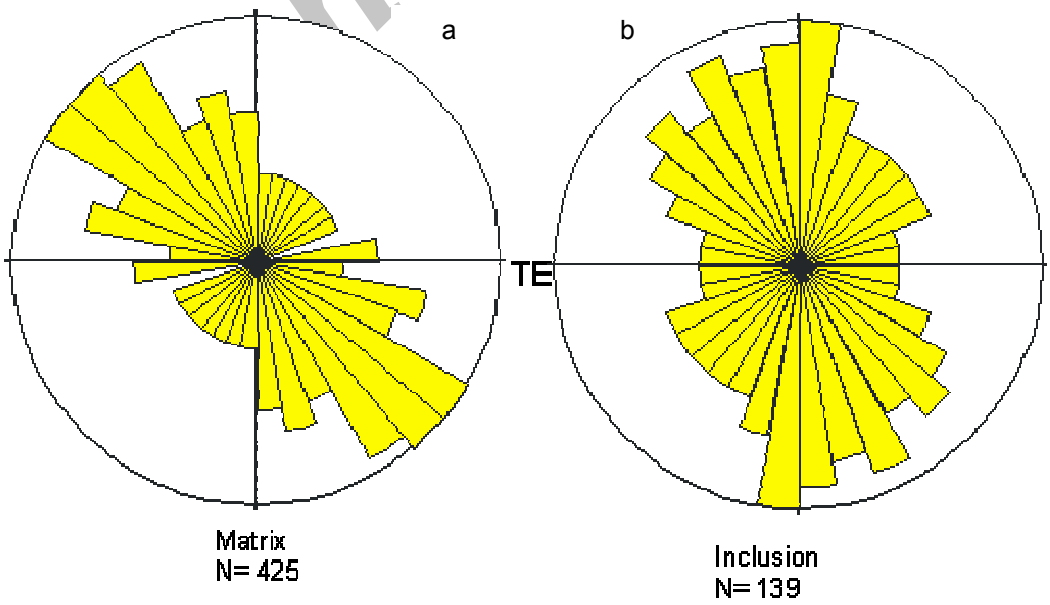


**Figure 5.** Long axes direction of quartz crystal in the matrix (a) and inclusions (b) of sample. Rose diagram perimeter representing 50% and 49% of the matrix and inclusions. N = number of crystals, TE = thin section edge.

**Crystallographic orientation of quartz crystals using EBSD**

The same areas of sample that were measured for SPO were selected for obtaining quartz crystallographic orientation data. To avoid local heterogeneity effects on the matrix-quartz crystallographic orientation, matrix quartzes were measured in quartz domains away from porphyroblasts. Quartz crystallographic orientation fabrics have been measured in an andalusite porphyroblast (Fig. 6a), and a part of the matrix (Fig. 6b). The results of texture analyses of quartz crystals are shown in Fig. 7. The c and a- axes of quartz orientations (in the andalusite and the matrix) are plotted as pole figures and contour diagrams [12]. There is no significant difference between the quartz crystallographic orientation in the andalusite porphyroblast and the matrix. Quartz crystals in both types show random crystallographic orientation distributions. It should be noted that each diagram has the kinematic Y-axis in the centre of the net, the Z-axis at the top and the X-axis at the intersection of the equatorial axis with the perimeter of the net.

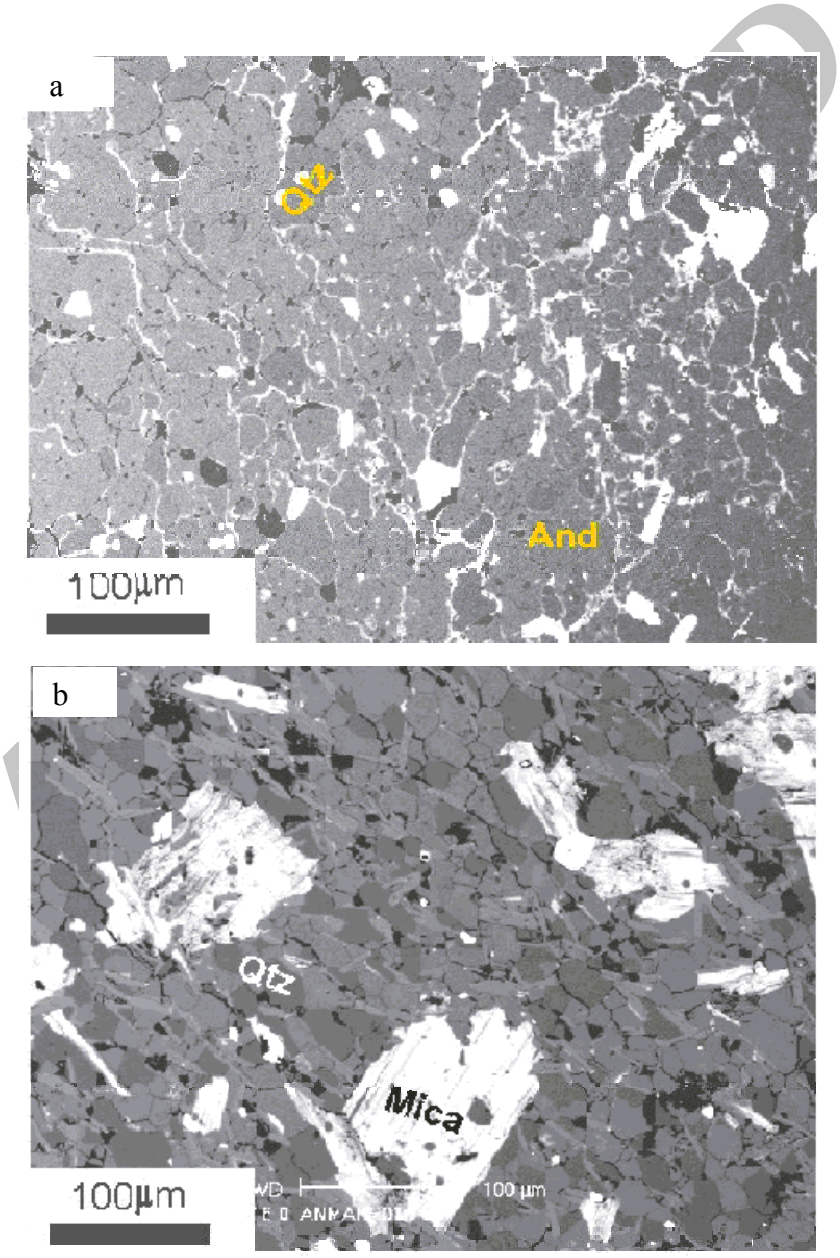


**Figure 6.** BSE images show the local of SPO and EBSD measurements of quartz crystals in inclusions (a) and the matrix (b). Qtz = quartz, And = andalusite

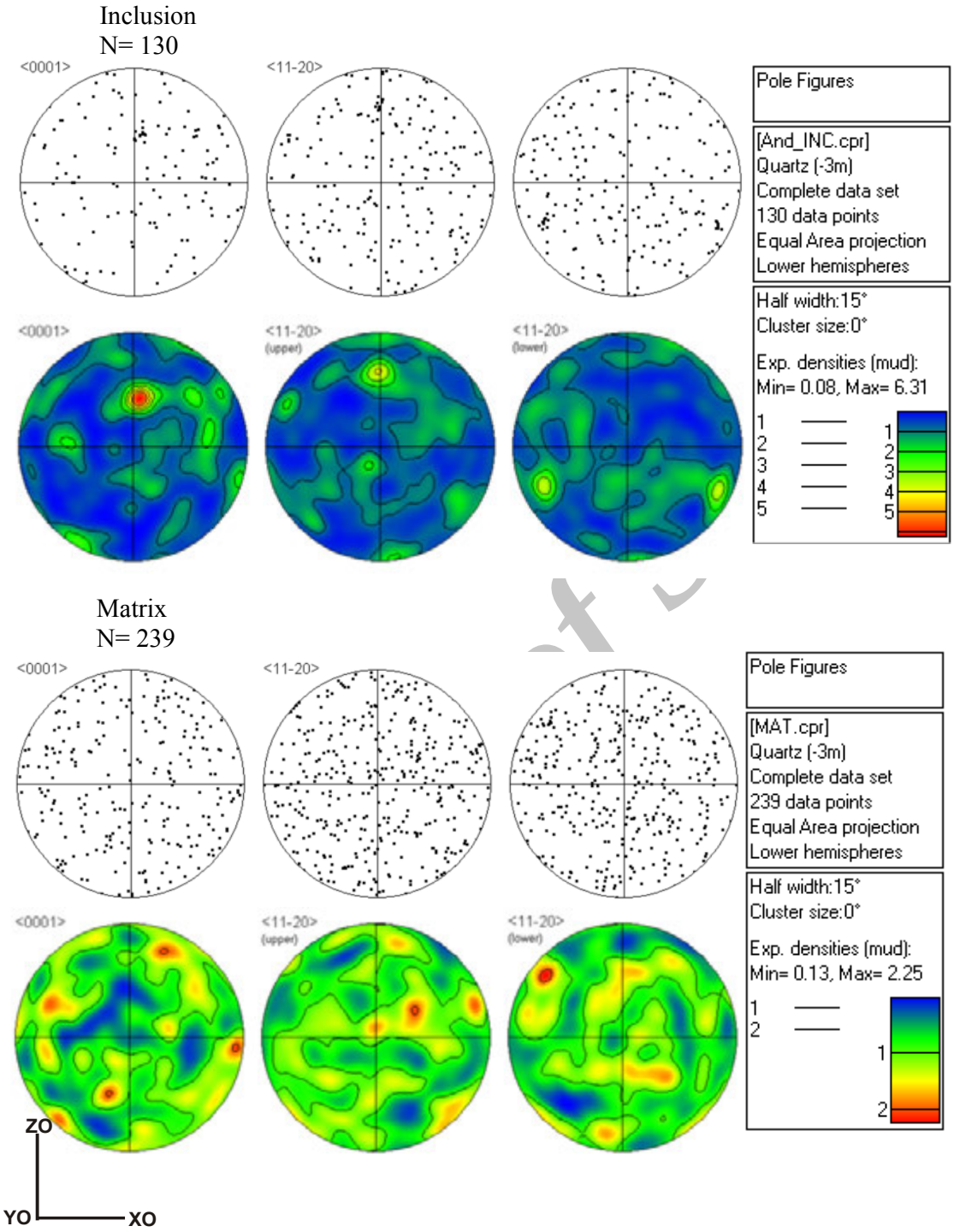


**Figure 7.** Quartz crystallographic orientations in both areas of the matrix and inclusions are plotted as pole figures and contour diagrams in <0001> and <11 20> directions in steronets of lower hemisphere of equal area projection, which were obtained manually. Kinematic reference is shown as ZO, YO, XO. N = number of grains

## Discussion

### Quartz SPOs

Long-axes of quartz grains do not show strong shape preferred orientation in a rose diagram (Fig. 5a). The question is, what mechanism controls the SPO of quartzes? Jessell and Bons [13] have listed processes that may affect the SPO of non-platy minerals (e.g. quartz):

1- Intra-crystalline processes;

- Dislocation glide, Twinning, Climb, Nabarro-Herring Creep and Kinking can lead to internal

deformation of individual grains, and hence of grain boundaries.

- Cracking- leads to generation of new grain boundaries; their orientation can be either crystallographically controlled or controlled by the orientation of the stress field, or some combination of both.
- Rotation recrystallisation- newly formed subgrains are typically fairly equant, so if these become sufficiently reoriented to become new grains, they will degrade the grain shape foliation.

2- Grain boundary migration

- Grain boundary migration (GBM) typically reduces the strength of the grain shape foliation, either during deformation, when dislocation density contrasts drive GBM or after deformation where in addition the surface energy driving force may be important.
- Coble creep- can lead to change of shape of individual grains, and hence of grain boundaries.

All above mechanisms are related to the amount of deformation. If it is accepted that the very weak schistosity of the sample was caused by deformation, then weak SPO in the matrix quartz crystals can be related to (1) GBM in granoblastic texture of quartzes that reduces SPO and (2) non-quartz crystals (e.g. mica in Fig. 6) at the junctions of quartz crystals that may control the SPO of quartzes.

When the quartz crystals were trapped by andalusite, the metamorphic condition was static (Buchan Type), because temperature was the dominant factor. In this period stress had minimum role to change the shape of quartz crystals. Therefore weak shape orientations of quartz inclusions in the andalusite porphyroblast can be explained by this mechanism.

**Quartz CPOs**

What causes the random crystallographic orientation of matrix and quartz crystals inclusion in sample? The crystallographic orientations of crystals may relate to (i) lattice rotation, (ii) grain boundary migration and (iii) diffusion processes [e.g. 13-18]. Lattice rotation might be caused by dislocation glide, twinning, kinking, rotation recrystallization or grain rotation. These mechanisms produce strong CPO in quartzes. Hirth and Tullis [16] have explained that the glide of dislocations on slip planes generally leads to the reorientation of the crystal lattice, which causes CPO. Jessell and Bons [13] have suggested that at higher temperatures, many grains will deform, since the critical resolved shear stress of all slip systems goes down with increasing temperature, but at low temperatures (sample), grains tend not to deform at all and tend to be preserved as augen grains. Because quartz has low dislocation densities, diffusion creep could explain the random crystallographic orientation of quartz crystals. Diffusion processes will happen when individual atoms or groups of atoms produce a net change in the shape of body [14]. Twiss and Moores [19] have stated that in this process, deformation takes place by the actual transfer of material from areas of high compressive stress to areas of low compressive stress. It may result from the diffusion of point defects through a crystal lattice (Nabarro-herring Creep), or diffusion of atoms or ions along grain boundaries (Coble Creep), or diffusion of dissolved components in a fluid along the grain boundaries (Solution Creep). Diffusion creep will not produced strong CPO in quartz crystals [18].

**Deformation mechanisms**

The weak mica foliation around cordierite porphyroblasts may reflect thermal history effect, without significant effects of deformation. Vernon [20] has explained that localised deformation can be expected during contact metamorphism. He notes that stages can be caused by (1) bulk volume changes due to thermal expansion of the aureole during heating, leading to unequal contraction in different directions during cooling; (2) volume changes between solid reactants and products in porphyroblast-producing reactions; and 3) deformation due to the intrusion. The $D_3$ deformation event occurred after the peak of metamorphism and was responsible for the folding of Buchan isograds around the 'Turriff Syncline' [7]. Hence, the weak SPO and lack of CPO of matrix quartzes could be related to the weak $D_3$ deformation. The similarity of the SPO and CPO of both matrix and inclusion quartzes suggest that (i) quartz inclusions are a relic of the rock texture existing before and during porphyroblast growth and (ii) non-selective trapping of the matrix quartzes in andalusite porphyroblasts. As was shown in Fig. 7, quartz inclusions were not controlled crystallographically by andalusite porphyroblasts, because the crystallographic orientation of quartz inclusions is not consistent.

**Conclusion**

Quartz crystals in the matrix and inclusions have inequant to slightly equant shapes. They show weak SPO that are sub-parallel to each other. The weak SPO in quartz crystals of sample can be related to (1) GBM of quartzes and (2) non-quartz

crystals (e.g. mica) at junction of quartz crystals. The latter may control the SPO of quartzes in the matrix.

The lack of CPO of quartz crystals in the matrix can be explained by (i) absence, or low amounts of strain in the rock that is experienced only low temperature and pressure and (ii) diffusion creep. The random crystallographic orientation of quartz inclusions may confirm non-selective orientations of the matrix quartzes by andalusite pophyroblast during growth.

**Acknowledgements**
The authors acknowledge the financial support from Ministry of Science, Research and Technology of IRAN.

**References**

[1] Chinner G. A., *"The distribution of pressure and temperature during Dalradian metamorphism*", Journal of the Geological Society, London. 122 (1966) 159-86.

[2] Harte B. and Johnson, M. R. W., "*Metamorphic history of Dalradian rocks in Glens Clova, Esk, and Lethnot, Angus, Scotland*", Scott. J. Geol. 5 (1969) 58-80.

[3] Atherton M. P., "*The metamorphism of the Dalradian rocks of Scotland*". Scott. J. Geol. 13 (1977) 331-370.

[4] Hudson N. F. C., "*Regional metamorphism of some Dalradian pelites in the Buchan area, N. E. Scotland*", Contrib. Mineral. Petrol. 79 (1980) 39-51.

[5] Dempster T. J., Hudson N. F. C. & Rogers, G., "*Metamorphism and cooling of the NE Dalradian*". Journal of the Geological Society, London, 152(1995) 383-390.

[6] Johnson M. R. W., "*Some time relations of movement and metamorphism in the Scottish highland*". Geologie Mijnb. 42(1963) 121-142.

[7] Read H. H., "*The Banff nappe: an interpretation of the structure of the Dalradian rocks of northeast Scotland*". Proc. Geol. Ass. 66(1955) 1-29.

[8] Rahimi-Chakdel, A., Boyle, A. P. and Prior, D. J. *Quartz deformation adjacent to a mid-crustal shear zone, the Renvyle-Bofin Slide, Connemara, western Ireland*. 16th Conference on Deformation mechanism, Rheology and Tectonics held 27 September-2 October at Milan, Italy, (2007)176.

[9] Rahimi-Chakdel A., Boyle A. P. and Prior D. J., "*Quartz deformation mechanisms during Barrovian metamorphism: Implications from crystallographic orientation of different generations of quartz in pelites",* Tectonophysics. 427(2006) 15-34.

[10] Prior D. J. & Wheeler J., "*Feldspar fabrics in a greenschist facies albite-rich mylonite from electron backscatter diffraction*, Tectonophysics. 303(1999) 29-49.

[11] Trimby, P. W. & Prior, D. J., "*Microstructural imaging techniques: a comparison between light and scanning electron microscopy*. Tectonophysics, Vol. 3031999., 71-81 pp.

[12] Peternell M., Hasalová P., Wilson C. J. L., Piazolo S. and Schulmann K. *Evaluating quartz crystallographic preferred orientations and the role of deformation partitioning using EBSD and fabric analyser techniques. Journal of Structural Geology,* 32 (2010) 803-817.

[13] Jessell M.W. & Bons, P.D., *The numerical simulation of microstructure. In: de Meer, S., Drury, M.R., de Bresser, J.H.P. & Pennock, G.M. (eds.) Deformation Mechanisms, Rheology and Tectonics: Current Status and Future Perspectives.* Geol. Soc, London, Spec. Publ. 200 (2002) 1137-147.

[14] Rutter E. H.**,** "*The kinetics of rock deformation by pressure solution*", Philosophical Transactions of the Royal Society of London. 283(1976) 203–219 pp.

[15] White S. H., *"The effects of strain on the microstructures, fabrics and deformation mechanisms in quartz"*. Philosophical Transactions of the Royal Society of London, 283 (1976). 69–86.

[16] Hirth G. and Tullis J. "*Dislocation creep regimes in quartz aggregates".* Journal of Structural Geology, 14 (1992) 145-159.

[17] Fliervoet T. F., White S. H. and Drury M. R. *Evidence for dominant grain boundary sliding deformation in greenschist-and amphibolite-facies polymineralic ultramylonites from the Redbank Deformed Zone, Central Australia*. Journal of Structural Geology**,** 19 (1997) 1495–1520.

[18] Fliervoet T. F., Drury M. R. and Chopra P. N. "*Crystallographic preferred orientations and misorientations in some olivine rocks deformed by diffusion or dislocation creep".* Tectonophysics**,** 303(1999) 1–27.

[19] Twiss R.J. and Moores E. M., "*Structural Geology*" W.F. Freeman and Company (2007).

[20] Vernon R. H., *"Evidence of syndeformational contact metamorphism from porphyroblast-matrix microstructural relationships"*, Tectonophysics, 158(1989) 113-126.